

## Estimating Pile Axial Bearing Capacity by $c$ - $\phi$ Derived from Pressuremeter Test

Tjie-Liong GOUW<sup>1</sup>

<sup>1</sup>Associate Professor, Universitas Katolik Parahyangan, Bandung, Indonesia

E-mail: [gtlooffice@gmail.com](mailto:gtlooffice@gmail.com)

**ABSTRACT:** Due to its rather brittle nature, retrieving undisturbed samples of Jakarta cemented greyish stiff clay, often found at a depth of 30 to 120m, is very difficult. Good and reliable effective shear strength parameters, i.e.,  $c'$  and  $\phi'$  values, obtained from triaxial test are hardly available. By modifying cavity expansion theory, Gouw (2017) was able to derive these effective shear strength parameters through Pressuremeter in situ test stress strain curve. It was found Jakarta cemented clay exhibiting a drained behaviour when loaded. Its effective cohesion,  $c'$ , values are linearly increasing with depths, averaging from around 95 kPa at 20 m to around 475 kPa at 100m depth, while its effective friction angle  $\phi'$  values are within 20° – 30°, averaging to around 24°. The values found to be similar to the values derived from CIU triaxial compression test from relatively good undisturbed samples. This paper presents the methodology in deriving the shear strength parameters and then applying the derived Pressuremeter  $c'$  and  $\phi'$  values to estimate the pile axial bearing capacity through finite element simulation and comparing it with the commonly known SPT method applied in Jakarta.

**Keywords:** Pressuremeter, modified cavity expansion theory, effective shear strength parameters, pile axial capacity

### 1. INTRODUCTION

By far, Pressuremeter test is the only known in-situ geotechnical testing device capable to generate a stress-strain curve of in-situ soils, somewhat similar to the stress-strain curve obtained from triaxial or direct shear test in soil laboratories. By simulating the Pressuremeter, hereinafter abbreviated as PMT, test through modification of cylindrical cavity expansion theory and matching the resulting stress strain curve with the actual PMT data curve, Gouw (2017) was able to derive effective shear strength parameters, i.e.,  $c'$  and  $\phi'$  values, of Jakarta cemented stiff clay. His research showed that Jakarta cemented clay, known of its rather brittle nature, exhibiting a drained behaviour when loaded under the PMT test. The effective cohesion,  $c'$ , values were found to be linearly increasing with depths, averaging from 95 kPa at 20 m depth to around 475 kPa at 100 m depth, while its effective friction angle  $\phi'$  values are within 20°–30°, averaging to around 24°. The values found to be similar to the values derived from CIU triaxial compression test from relatively good undisturbed samples. This paper presents the PMT testing principle, the traditional PMT parameters, the modified cavity expansion formulas used, a case study in deriving  $c$  and  $\phi$  of Jakarta cemented clay, and application of the values obtained to estimate pile axial bearing capacity through finite element simulation, finally comparing the result with the commonly known SPT method applied in Jakarta local practice.

### 2. PRESSUREMETER TEST AND ITS PARAMETERS

Pressuremeter test is conducted by inserting a cylindrical membrane into a carefully prepared borehole to a determined test depth where the cylindrical membrane is then pressurized against the borehole wall and the subsequent volume expansion (Menard PMT) or the radial expansion (OYO PMT) of the cylindrical membrane is measured. Figure 1 shows the schematic diagram of PMT.

If the pressure is applied by pumping de-aired water into the cylindrical membrane, the actual pressure or stress acting on the borehole wall needs to be corrected against membrane resistance and against the hydrostatic pressure from the manometer level to the centre of the membrane. In Menard PMT the volume of expansion is corrected against the expansion of the hose to deliver the water from the control unit to the membrane. In OYO PMT, also known as Elastmeter, the radius of expansion is corrected against the reducing membrane thickness when pressurised.

The corrected volume or radius is then converted into radial strain of the borehole wall. The resulting corrected radial stress strain data is then plotted. Figure 2 shows the typical stress strain curve obtained from PMT test.

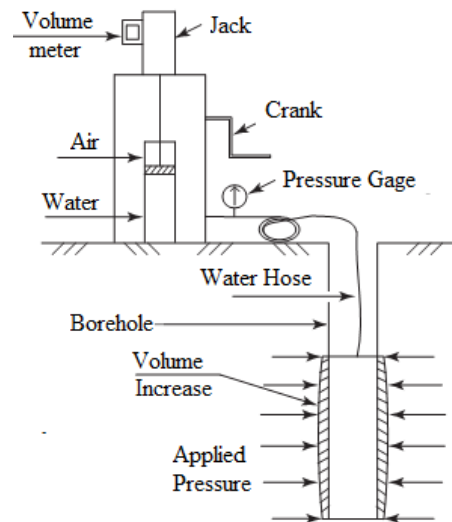


Figure 1 Schematic Diagram of Pressuremeter Test (Briaud, 2013)

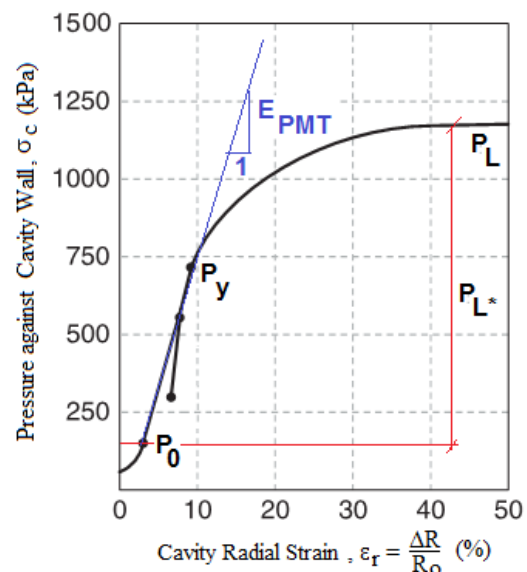


Figure 2 Pressuremeter Typical Test Graph (modified after Briaud, 2013)

Traditionally six parameters are obtained from the PMT stress-strain curve, i.e.:  $P_o$ ,  $P_y$ ,  $P_L$ ,  $K_m$ ,  $E_m$ , and  $G$  (Baguelin et al, 1972, 1978; Gambin, 1980, 1995; Gambin and Frank, 2009; Clayton et al, 1982; Briaud, 1992; Clarke, 1995). The parameters are described below (refer to Figure 2 for some notations):

- Horizontal pressure,  $P_o$ , is the pressure when the membrane first touches the borehole wall, i.e. first point at the beginning of linear or elastic part of PMT curve. This pressure is interpreted as soil total horizontal pressure at rest, i.e.,

$$P_o = \sigma'_{vo} k_o + u_o \quad (1)$$

$$\sigma'_{ho} = \sigma'_{vo} k_o = P_o - u_o \quad (2)$$

where  $\sigma'_{vo}$  is vertical effective pressure,  $\sigma'_{ho}$  is horizontal effective pressure,  $k_o$  is at rest horizontal earth pressure coefficient,  $u_o$  is hydrostatic groundwater pressure.

- Yield pressure,  $P_y$ , is the end of the linear curve and the beginning of the non-linear or plastic part of the PMT curve,
- Limit pressure,  $P_L$ , is the ultimate pressure of PMT curve where soil start to 'flow', i.e. radial strain keeps on increasing at relatively constant pressure. In practice, limit pressure is hardly achieved, and to obtain this  $P_L$  value, the test curve must be extrapolated in a logarithmic plot as shown in Figure 3 below,

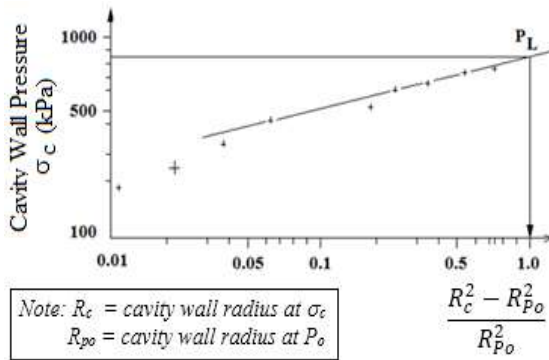


Figure 3 Extrapolation of PMT Test Data to Obtain  $P_L$  (Modified after Baguelin et al, 1978, Ghionna et al, 1981)

- Horizontal subgrade reaction,  $K_m$ , obtained through linear part of the test curve, i.e.:

$$K_m = \frac{\Delta P}{\Delta R} = \frac{P_y - P_o}{R_{Py} - R_{Po}} \quad (3)$$

where  $R_{Py}$  is cavity radius at  $P_y$  and  $R_{Po}$  is cavity radius at  $P_o$ .

- Soil deformation or stiffness modulus,  $E_m$  :

$$E_m = (1+v) \frac{R_{Po} + R_{Py}}{2} K_m \quad (4)$$

where  $v$  is Poisson ratio of the soil, usually taken as 0.33.

- Shear Modulus,  $G$  :

$$G = \frac{E_m}{2(1+v)} \quad (5)$$

### 3. MODIFIED CAVITY EXPANSION FORMULAS

The cavity expansion theory used in deriving the shear strength parameters from PMT test curve is modified from Mecsi work (Mecsi, 2013) which is elaborated below.

The expansion of cylindrical cavity can be divided into elastic and plastic zone as illustrated in Figure 4. By using Mohr Coulomb failure criterion and radial stress vs modulus of deformation, depicted in Figure 5, Mecsi derive equations to calculate the cohesion,  $c$ , and friction angle,  $\phi$ , of soils, from PMT test data. His equations are:

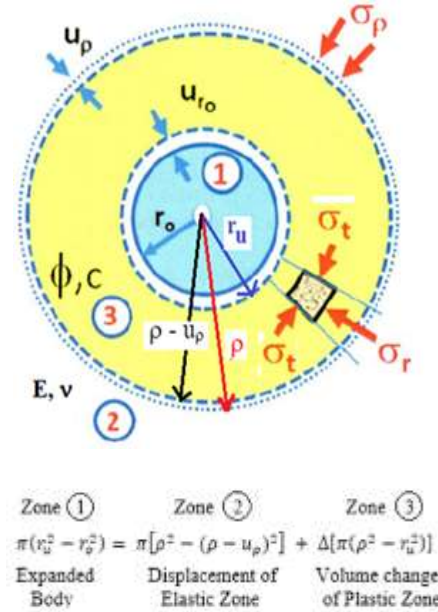


Figure 4 Cylindrical Cavity Expansion Zone (Modified after Mecsi, 2013)

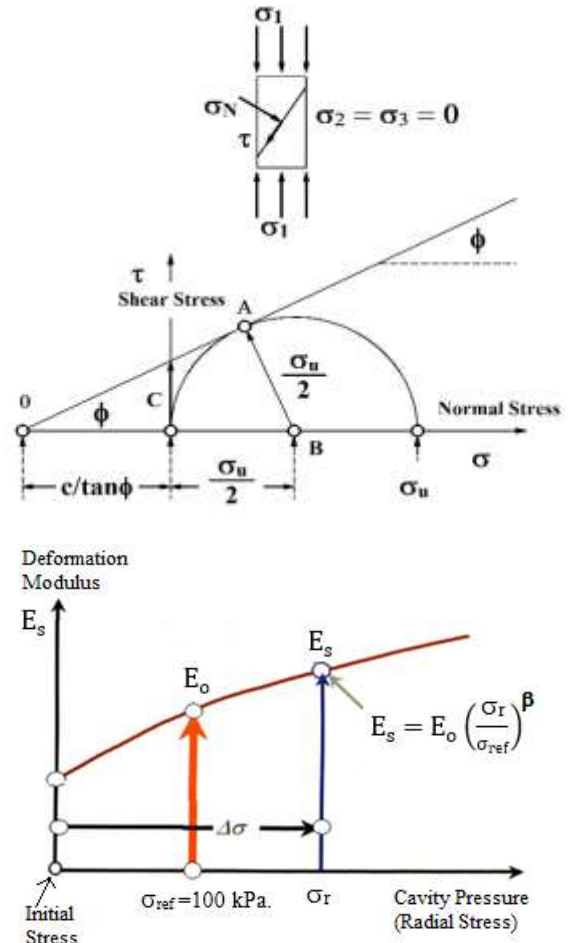


Figure 5 Mohr Failure Criterion and Modulus of Deformation Relationship (Modified after Mecsi, 2013)

$$= \frac{2}{\sqrt{\pi}} \quad (6)$$

$$= \frac{1-}{1+} \quad (7)$$

$$E_s = E_o \left( \frac{\sigma_r}{\sigma_{ref}} \right)^\beta \quad (8)$$

where  $E_s$  is deformation modulus at a cavity pressure of  $\sigma_r$ ,  $E_o$  is deformation modulus at a reference pressure  $\sigma_{ref} = 100$  kPa as shown in Figure 5, coefficient  $\beta$  is rigidity index.

The radius where the soil is still in compression is defined as radius of compression (plastic) zone,  $\rho$ , and formulated as:

$$\rho = r_c \left( \frac{\sigma_r + c \cdot \cot \phi}{\sigma_\rho + c \cdot \cot \phi} \right)^{\frac{1 + \sin \phi}{2 \sin \phi}} \quad (9)$$

where  $r_c$  = cavity radius at cavity pressure  $\sigma_r$  and  $\sigma_\rho$  is horizontal or radial stress at boundary of compression zone which is defined as:

$$\sigma_\rho \approx \frac{\sigma'_{ho}}{\beta} \left[ 1 + \xi - \sqrt{(1 + \xi)^2 - 2\beta(1 - \xi)2\beta\xi \frac{\sigma'_u}{\sigma'_{ho}}} \right] + \sigma'_{ho} \quad (10)$$

The radial stress inside the compression zone (at radius  $r \leq \rho$ ) is:

$$\sigma_r = \left( \sigma_\rho + \frac{c}{\tan \phi} \right) \cdot \left( \frac{\rho}{r} \right)^{\frac{2 \sin \phi}{1 + \sin \phi}} - \frac{c}{\tan \phi} \quad (11)$$

The radial stress outside the compression zone (at radius  $r > \rho$ ) is:

$$\sigma_r = (\sigma_\rho - \sigma'_{ho}) \cdot \left( \frac{\rho}{r} \right)^2 + \sigma'_{ho} \quad (12)$$

The induced radial strain,  $\varepsilon_r$ :

$$\Delta \varepsilon_r = \frac{\sigma_{ref}}{(1 - \beta)E_o} \left[ \left( \frac{\sigma_r}{\sigma_{ref}} \right)^{1 - \beta} - \left( \frac{\sigma'_{ho}}{\sigma_{ref}} \right)^{1 - \beta} \right] \quad (13)$$

The induced radial displacement  $U_r$ :

$$\Delta U_r = \frac{\Delta \varepsilon_r(i-1) + \Delta \varepsilon_r(i)}{2} (r_{(i)} - r_{(i-1)}) \quad (14)$$

With the above formulas, it is supposed to be able to derive the  $c$  and  $\phi$  of clayey soils by matching PMT test data curve with the calculated radial stress strain curve, i.e. matching  $\sigma_r$  vs  $\varepsilon_r$  plot from PMT against  $\sigma_r$  vs  $\varepsilon_r$  plot from the above cavity expansion formulas.

Gouw (2017) found that the above formulas could not match PMT data curve of Jakarta cemented stiff clay, especially in the plastic phase of the curve, i.e. the part after yield pressure  $P_y$ . To match the test data curve, many trial and error were done. However, every trial could only partially match the PMT data curve and gave different set of  $\beta$ ,  $c$  and  $\phi$  values, i.e. no unique values could be obtained. On the same test data curve, each of the diagram in Figure 6 shows different values of rigidity index and  $c - \phi$  values! By modifying the deformation modulus function, i.e. modifying equation (8), Gouw (2017) was finally able to match the PMT test data curve and derive a more consistent values of  $c - \phi$  of Jakarta cemented stiff clay. The modified formula is as follows:

- When PMT stress level is still within the linear range, i.e. within  $P_o$  to  $P_y$ , equation (8) needs to be modified into:

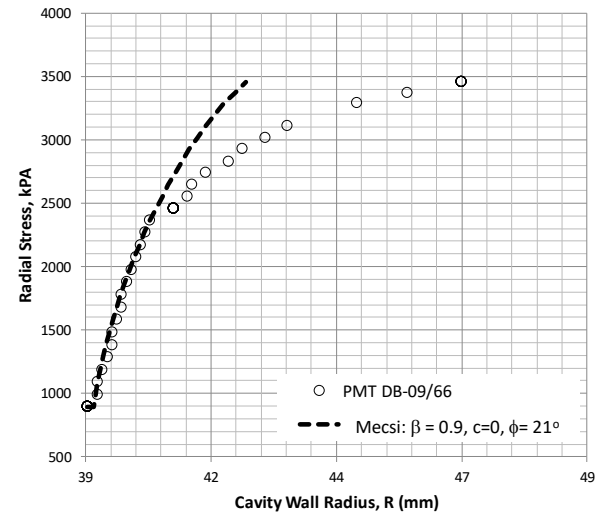
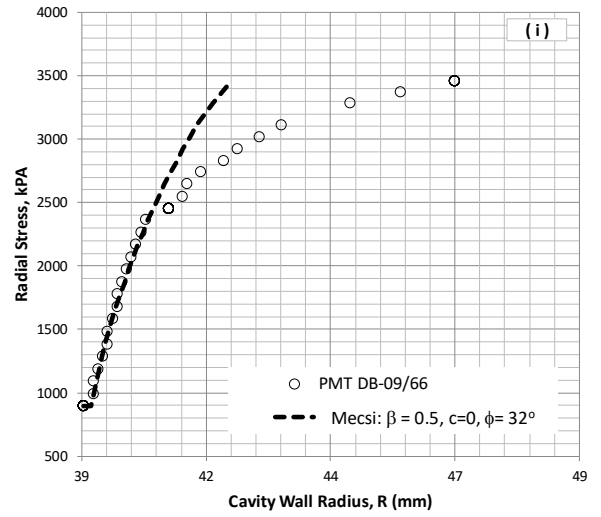


Figure 6 No Unique  $c - \phi$  values obtained by Mecsi Formulas

$$E_s = E_o \left( \frac{\sigma_c}{100} \right)^{0.5} \quad (8a)$$

- When PMT stress level is above yield pressure  $P_y$ ,

$$E_{sy} = E_{y0} \left( \frac{\sigma_{cy}}{P_y} \right)^{a_{ye}} \rightarrow E_{sy} = m_y E_o \left( \frac{\sigma_{cy}}{P_y} \right)^{a_{ye}} \quad (8b)$$

- $E_s$  = elastic soil deformation modulus at cavity pressure of  $\sigma_c$
- $E_o = E_m$  = pressuremeter modulus as defined in equation (4)
- $E_{sy}$  = plastic deformation modulus =  $\sigma_{cy}/\varepsilon_y$  = cavity pressure at plastic part divided by its corresponding strain (from Pressuremeter test data)
- $E_{y0} = m_y \cdot E_o = m_y \cdot E_m$
- $m_y$  = yield factor
- $\sigma_{cy}$  = cavity pressure at and above yield pressure
- $a_{ye}$  = rigidity factor after yield pressure

To find both  $m_y$  and  $a_{ye}$ , equation 8b is normalized as follows:

$$\frac{E_{sy}}{E_m} = m_y \left( \frac{\sigma_{cy}}{P_y} \right)^{a_{ye}} \quad (8c)$$

from PMT data calculate and plot  $E_{sy}/E_m$  vs  $\sigma_{cy}/P_y$ , the parameter  $m_y$  and  $a_{ye}$  can then be obtained by running power function regression analysis. Figure 7 shows one of the plotted test data. In this case,  $m_y = 0.6151$  and  $a_{ye} = -2.06$ . Once parameter  $m_y$  and  $a_{ye}$  are found, substitute these parameters to equation 8b.

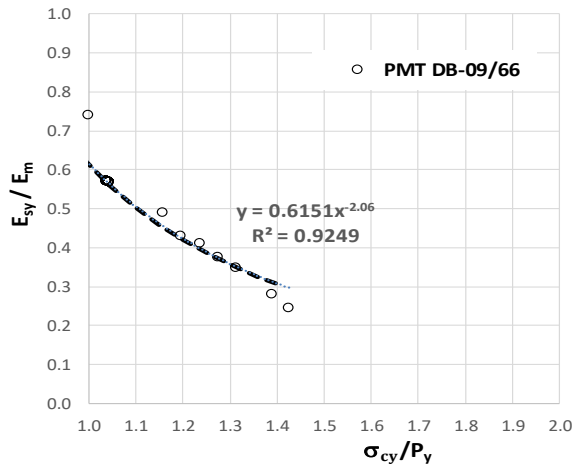


Figure 7 Finding  $m_y$  and  $a_{ye}$  from Pressuremeter Test Data

Figure 8 shows one of the results of PMT test curve matching with curve calculated from the modified equation (8), i.e. modified E function or modified cavity expansion model. The result shows that when the stiff clay is still in linear “elastic” range, the shear strength consists both cohesion and angle of internal friction (since the shear strength parameters are derived from Pressuremeter, it is notated as  $c_{PMT}$  and  $\phi_{PMT}$ ). However, once the soil entering non-linear plastic part, the stiff clay lost its cohesion ( $c_{YPMT} = 0$  kPa), and only the angle of internal friction  $\phi_{YPMT}$  is working. It is also found that the angle of internal friction remains constant throughout the elastic and plastic phase, i.e.  $\phi_{PMT} = \phi_{YPMT}$ . The same outcomes are found from all the PMT test data.

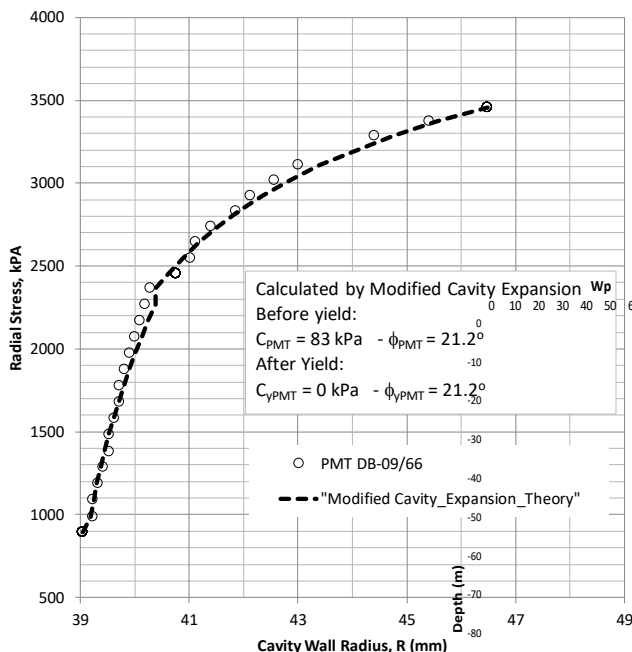


Figure 8 Good Match of PMT Test Data vs Modified Cavity Expansion Theory

#### 4. CASE STUDY ON JAKARTA CEMENTED CLAY

A case study was carried out at a project site at Bendungan Hilir, central Jakarta, where many high-rise buildings are located. The following field and laboratory testings were carried out:

- 21 deep borings carried out between 90 to 120 m depths. SPT tests were taken at every 2 to 3.5 m intervals.

- 20 pre-borehole Pressuremeter tests conducted at cemented stiff clay layers.
- A total of 123 undisturbed samples for laboratory index properties tests, triaxial UU, triaxial CIU and consolidation tests.

Figure 9 to 10 show index and engineering properties of the subsoil. Stiff clay layer is found below 20m depth, it exhibits an increasing SPT blow counts with depth, bulk unit weights vary within 16.5–18.5 kN/m<sup>3</sup> (Figure 9). Plasticity index are mostly within 20 to 60%, water contents fall near the plastic limits, with liquidity indices less than 0.30, an indication of stiff clay (Figure 10). Void ratios of the stiff clay are found to be within 0.70-1.30, it has specific gravity of around 2.63, and water content averaging around 35% (Figure 11).

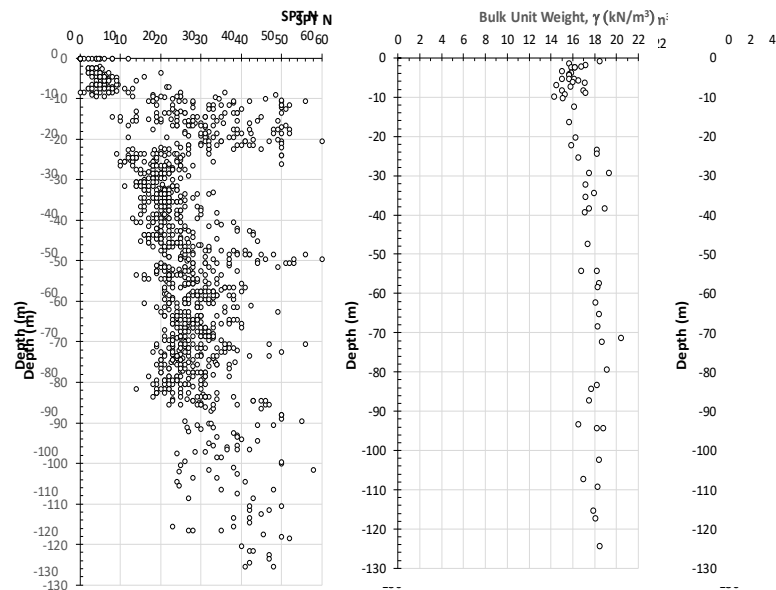


Figure 9 SPT Blow Counts and Bulk Unit Weight

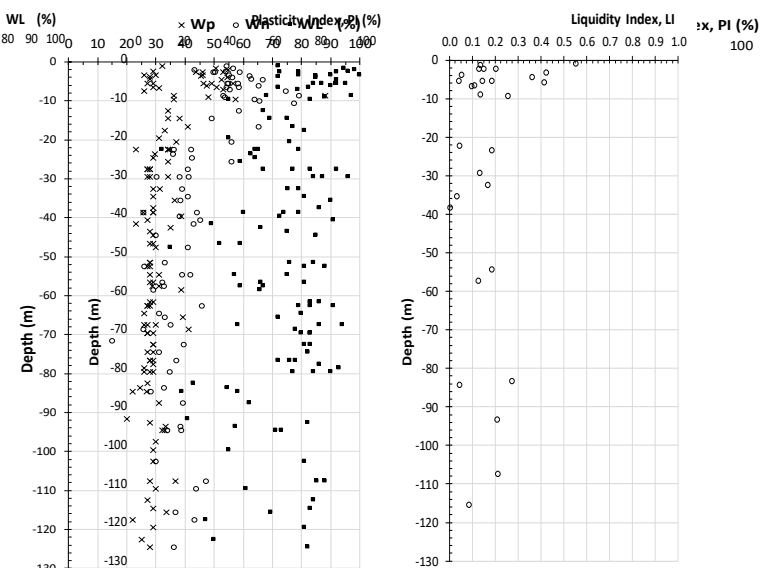


Figure 10 Atterberg Limits and Liquidity Indices

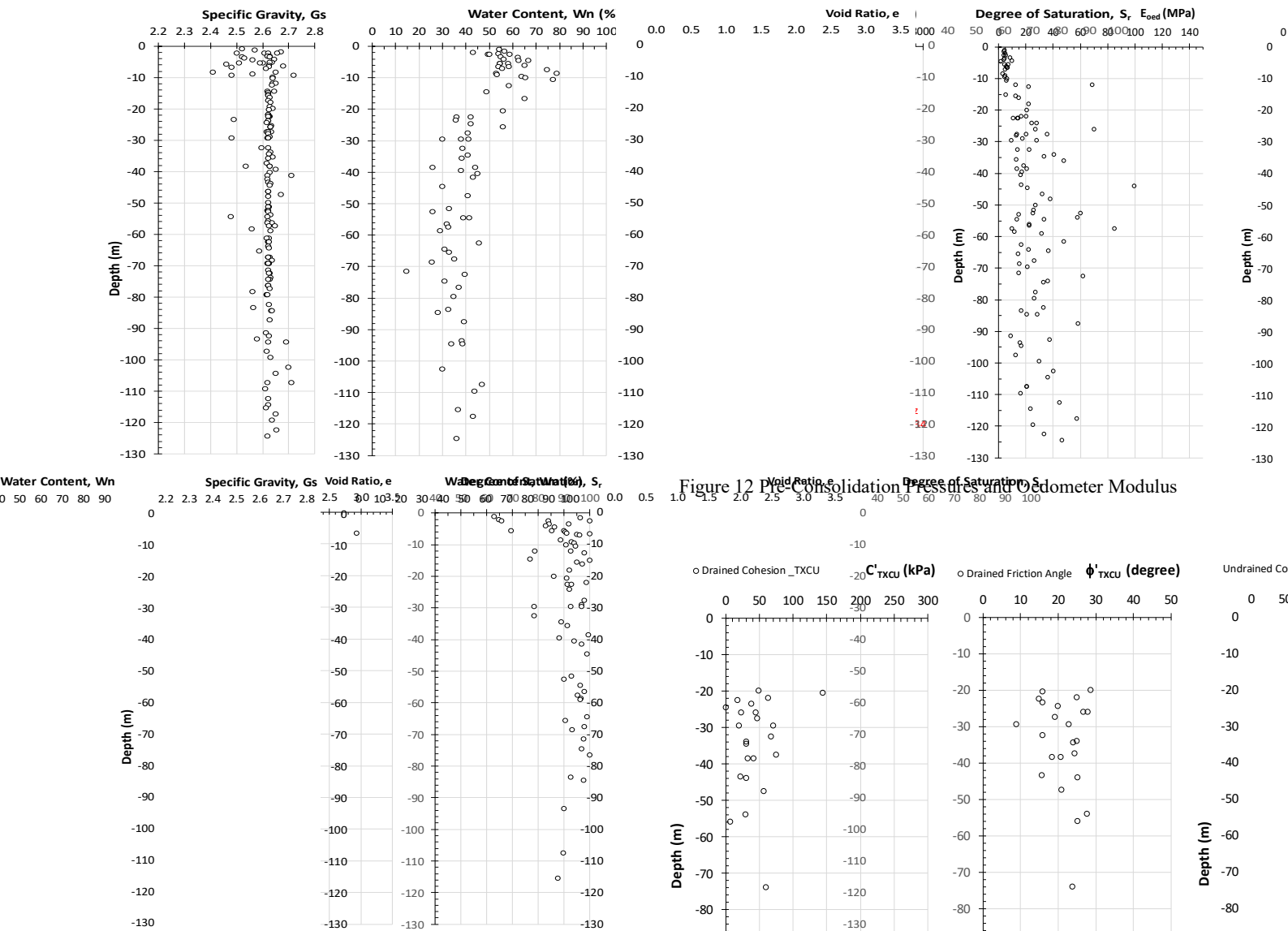


Figure 11 Specific Gravity, Water Content, Void Ratio and Degree of Saturation

Figure 12 shows the pre-consolidation pressure and oedometer modulus. The pre-consolidation pressures appear increasing with depth. Comparing with the corresponding effective stresses, the over consolidation ratio of the stiff clay layers is found to be in the order of 2.0. The effective and total shear strength obtained from triaxial CIU tests are shown in Figure 13.

Figure 14 shows typical PMT test data match reasonably well with the curve derived from the modified cavity expansion theory described above. The black triangular dots show the PMT test data point and the dashed red lines show the curve obtained from modified cavity expansion theory. With this matching of curve, the  $c$  and  $\phi$  values of the tested cemented stiff clay can be derived. Note that the notation of PMT DB-xx/yy in the graphs means the PMT test conducted at borehole no xx at depth of yy meter. Figure 15 shows the PMT parameters derived from the test data, all the notations on the graphs are as defined before. The effective horizontal stress  $\sigma'_{ho}$  is obtained by subtracting PMT total horizontal pressure  $P_o$ , with its corresponding hydrostatic groundwater pressure, as formulated in equation (2). It is important to show the value of effective horizontal stress here as it needs to be implemented in equations (10), (12), and (13).

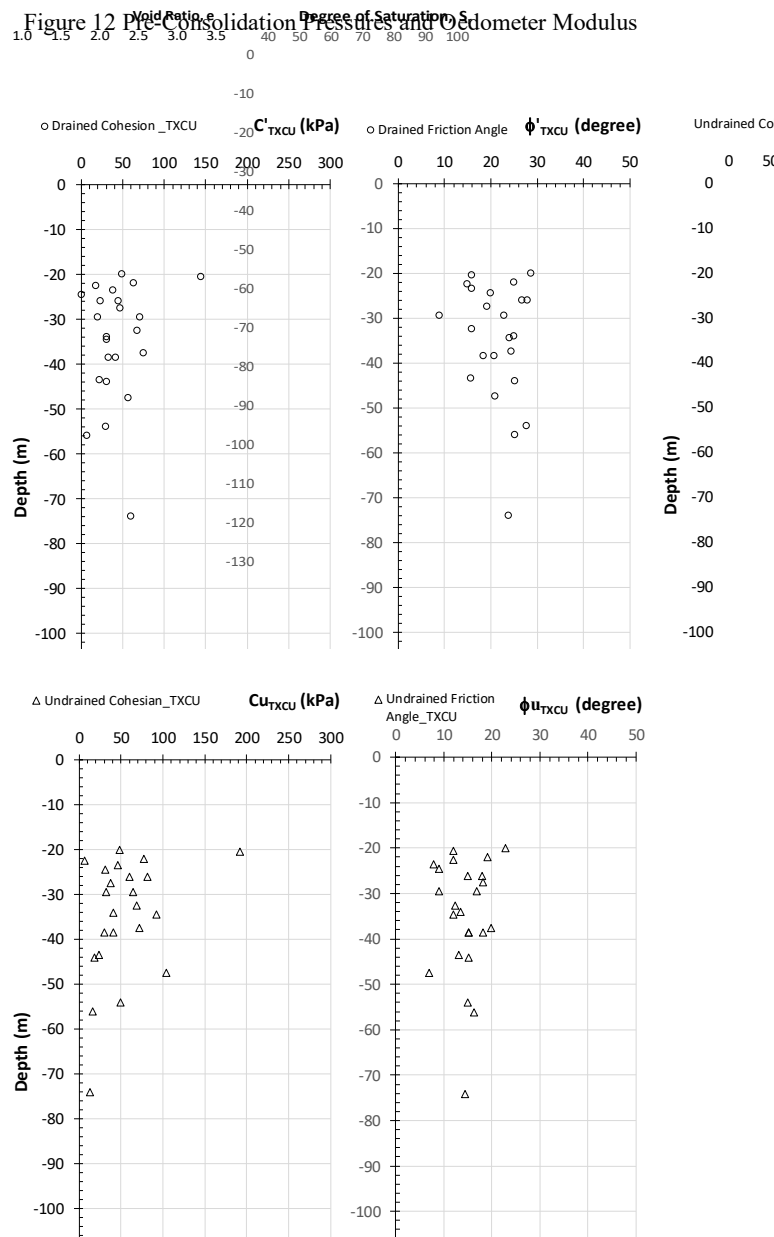


Figure 13  $c'$  -  $\phi'$  and  $c_u$  and  $\phi_u$  from Triaxial CIU Tests

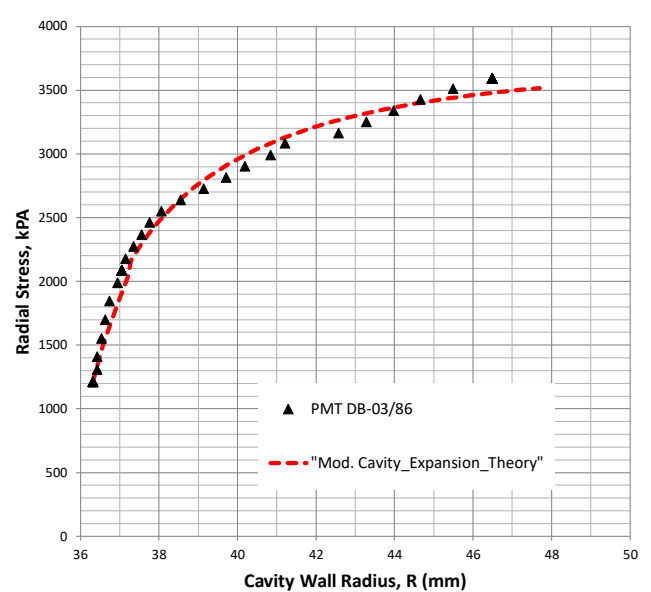
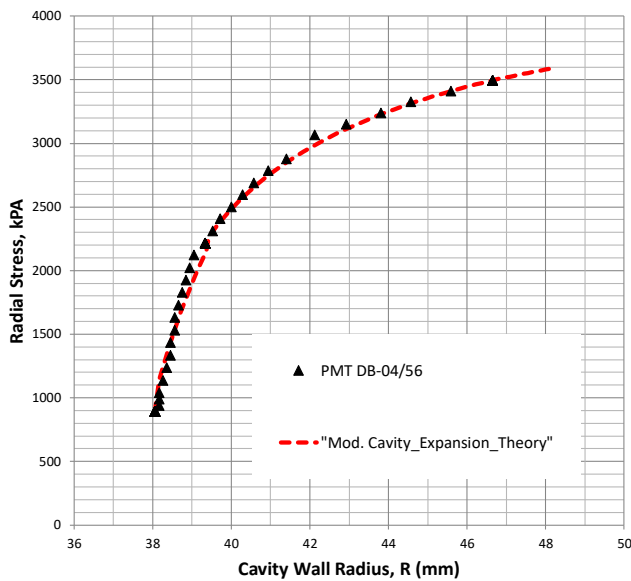
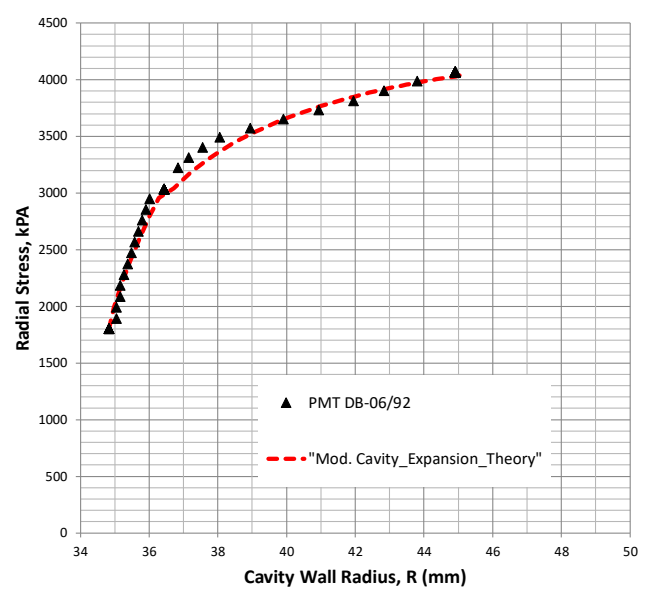
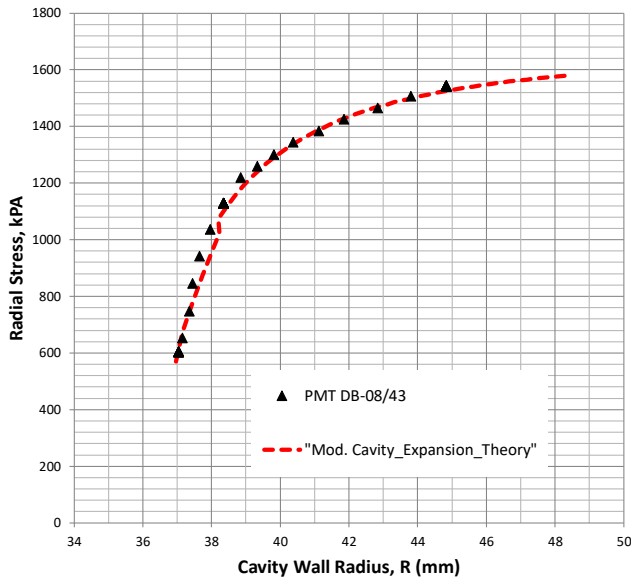
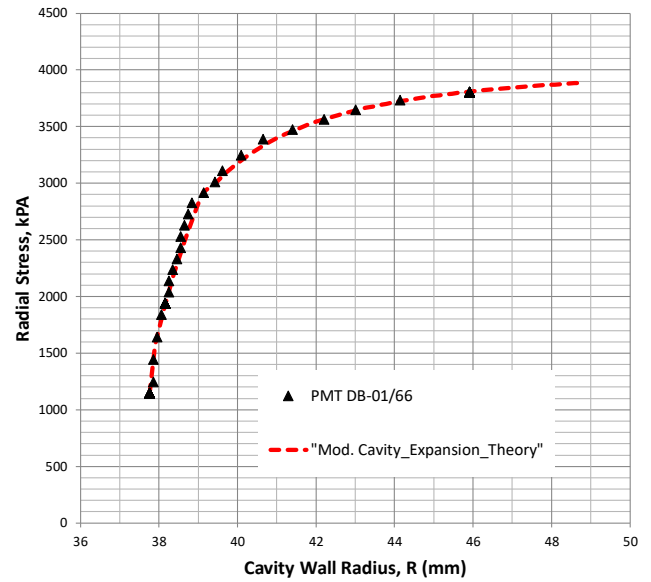
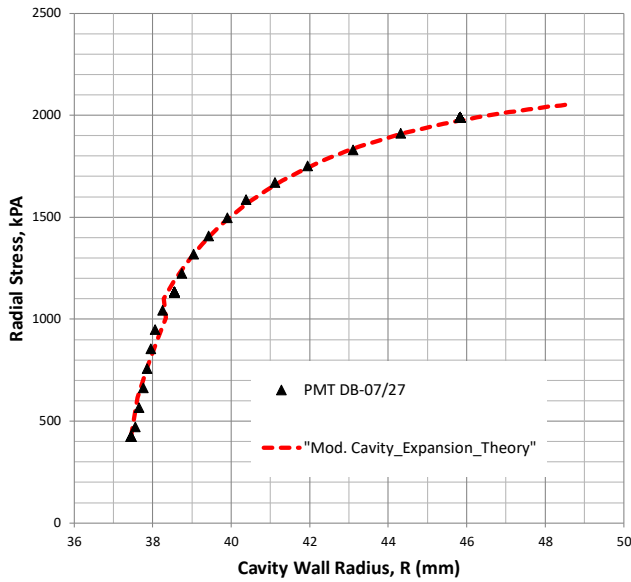


Figure 14a PMT Test Data Points (black triangular points) vs Modified Cavity Expansion Theory (dashed red line)

Figure 14b PMT Test Data Points (black triangular points) vs Modified Cavity Expansion Theory (dashed red line)



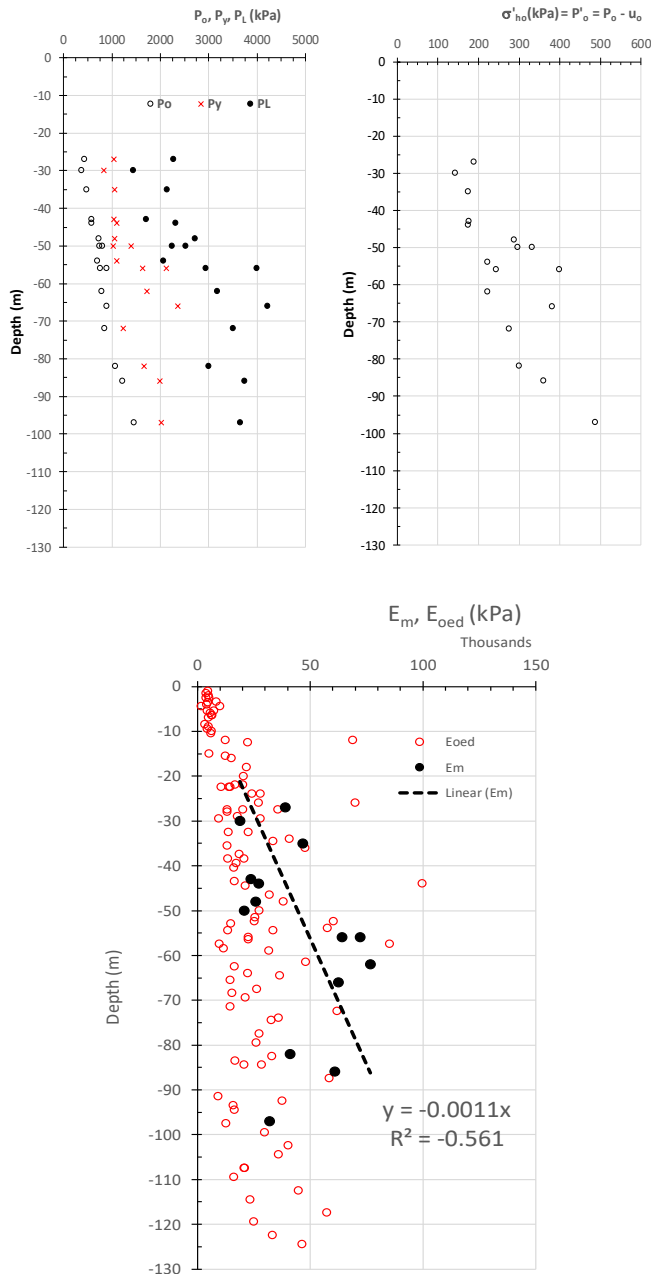


Figure 15 Pressuremeter Parameters and Oedometer Modulus

Figure 16 and 17 show the  $c$  and  $\phi$  values derived from PMT data, notated as  $c_{PMT}$  and  $\phi_{PMT}$ , plotted against effective (drained) and total (undrained)  $c - \phi$  from CU triaxial test, respectively. It can be seen the  $c - \phi$  values derived from PMT data by using modified cavity expansion give a clear existence of soil cohesion when the stress strain of the stiff clay is still within the linear “elastic” range, i.e.  $c_{PMT}$  and  $\phi_{PMT}$  are mobilized at the same time (since the  $c$  and  $\phi$  are derived from PMT, they are given PMT indices). However, once the stress level reaching and above its yield stress level the stiff clay losses the cohesion ( $c_{PMT} = c_{ultimate} = 0$ ), what remain thereafter is the angle of internal friction which remain constant throughout all the stress level ( $\phi_{PMT} = \phi_{peak} = \phi_{ultimate}$ ). The same outcomes are found from all the PMT test data. This means Jakarta stiff clay exhibits no dilation property ( $\phi_{peak} - \phi_{ultimate} = 0$ ).

Comparing Figures 16 and 17, from 27m to 97m depth the  $\phi_{PMT}$  values are within  $21^\circ - 33^\circ$  and these values fall within the drained angle of internal friction (Figure 16) rather than the undrained angle of internal friction (Figure 17) obtained from triaxial test. The results also show the cohesion parameter of Jakarta stiff clay increases with

depth, with a value of around 95 kPa at a depth of 20 m to 475 kPa at a depth of 100 m, and it is clearly higher than the values obtained from CU triaxial test, be the undrained or drained cohesion. The lesser values of cohesion from triaxial tests are generally attributed to the brittle nature of the Jakarta cemented stiff clay which tends to suffer micro cracks resulted from the sampling process by thin wall tube sampler and during the preparation of the samples in the laboratory. The higher values of  $c_{PMT}$  is attributed to the cemented nature of the Jakarta stiff clay.

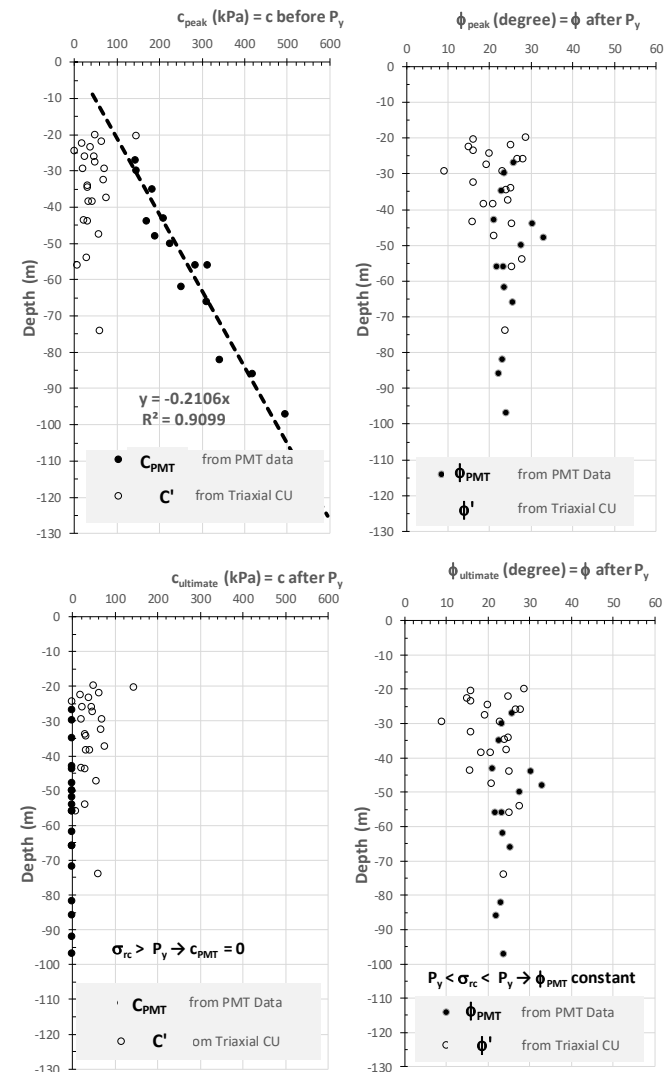


Figure 16  $c_{PMT}$  and  $\phi_{PMT}$  vs Triaxial Drained  $c' - \phi'$

From all the above phenomena, it can be concluded or at least postulated that for Jakarta stiff clay, at the initial stage of Pressuremeter test the soil is in partially or near drained cohesion, as the radial stress and strain reaches its yield pressure,  $P_y$ , the stiff clay is already in fully drained cohesion. The explanation is: at the initial stage, while the radial stress tends to reduce the soil volume, the concurrent induced tangential strain will expand the soil radially, therefore the soil is not in a fully compressive nature, but rather in a radial and tangential ring like shearing nature. Consequently, at this stage the soil at least is in a partially drained condition. At and beyond yield pressure, the induced tangential strain will be large enough to cause spacings within the clay particles move to a larger distance one another and possibly creates micro cracks within the soil structure, hence the clay start to lose its cohesion and left only with its angle of internal friction, at this stage the stiff clay is already in a fully drained condition. This postulated phenomenon is illustrated in Figure 18.

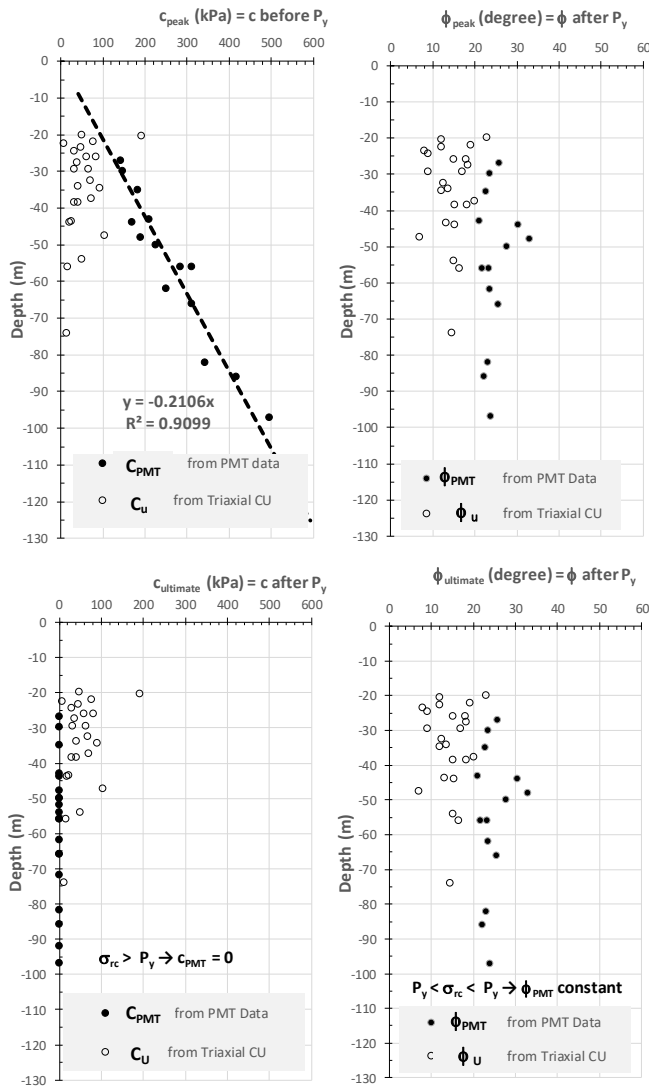


Figure 17  $c_{PMT}$  and  $\phi_{PMT}$  Triaxial Undrained  $c_u - \phi_u$

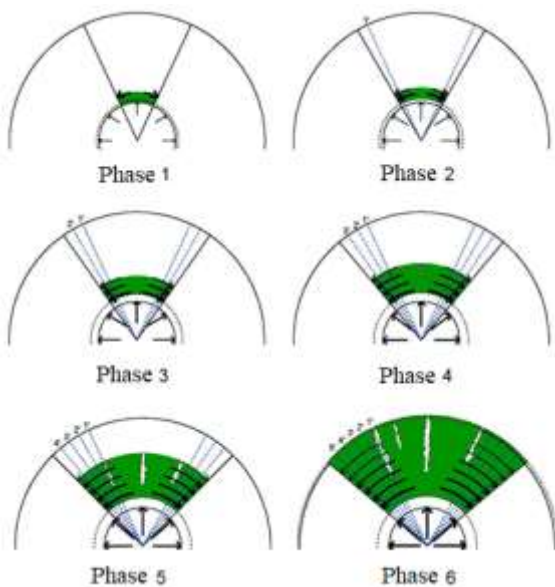


Figure 18 Radial Expansion causing Micro-cracks

As found above, the strength parameters of the Jakarta cemented stiff clay derived from the PMT tests,  $c_{PMT}$  and  $\phi_{PMT}$ , together with the PMT deformation modulus,  $E_m$ , are linearly increasing with depth and can be written as follows:

From 20 m to 100 m depth:

$$c_{PMT} \text{ (kPa)} = y \text{ (m)} / 0.2106 \quad (15)$$

$$E_{PMT} \text{ or } E_m \text{ (kPa)} = y \text{ (m)} / 0.0011 \quad (16)$$

where  $y$  is depth in m.

## 5. ESTIMATING PILE AXIAL CAPACITY

The shear strength and the deformation modulus of the stiff cemented clay obtained from PMT data are applied to estimate pile axial bearing capacity through finite element analysis by using the axisymmetric model in Plaxis 2D software. The input parameters are presented in Table 1. The finite element model is shown in Figure 19. Figure 20 shows the resulted pile load settlement curve. By applying the ultimate load criterion set in the Indonesian Geotechnical standard (SNI 8640:2017) which set the ultimate load as the load at pile head settlement of 4% pile diameter, the ultimate pile capacity can be estimated.

Table 1 Plaxis Input Parameters

Depth, $y$ (m)		Mohr Coulomb Soil Model				
from	to	$\gamma$ (kN/m <sup>3</sup> )	$c'$ (kPa)	$\phi'$ (deg)	$E'$ (kPa)	$\nu$
0	-10	16	10	20	5000	0.33
-10	-20	18	0	32	35000	0.33
-20	-100	18	$y / 0.2106$	24	$y / 0.0011$	0.33

Groundwater level = -15m

Pile Properties

- Modeled as linear elastic material
- Pile Diameter = 1.5 m
- Pile Depth = 70 m from ground surface

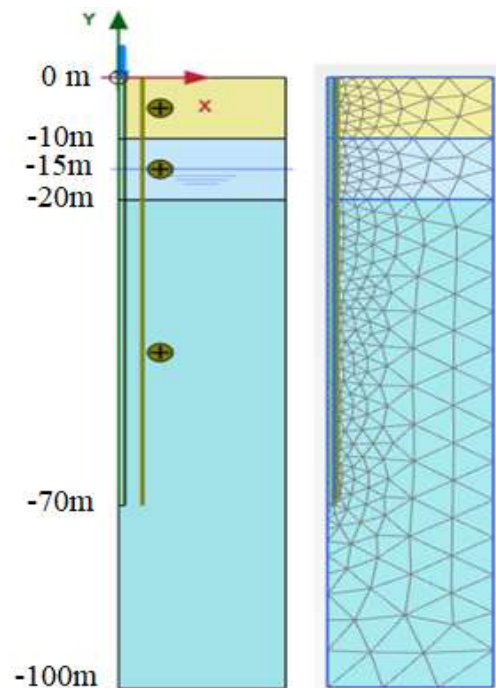


Figure 19 Plaxis Finite Element Model



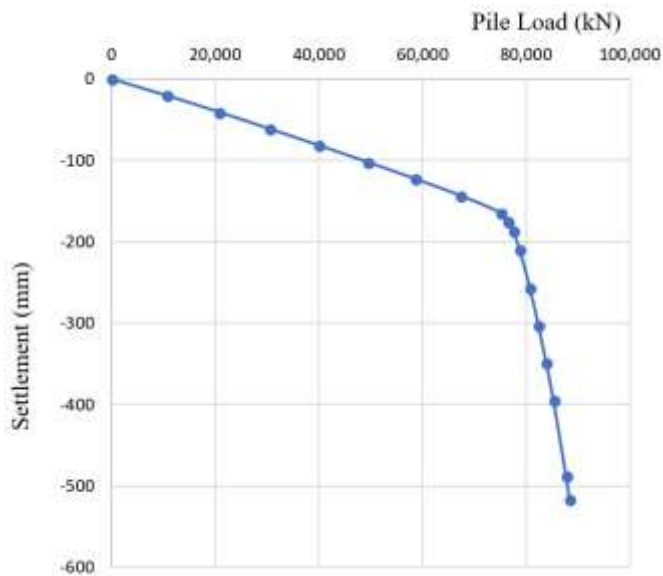


Figure 20 Pile Load Settlement from FEM Analysis

4% of 1.5m pile diameter is 60 mm pile head settlement, from figure 19, it can be found that the ultimate capacity of the pile is:

$$Q_{ult\_PMT} = 30,395 \text{ kN}$$

Figure 20 shows the idealised SPT profile to calculate the pile axial bearing capacity from the following formula:

$$Q_{ult} \text{ (kN)} = m N_s A_s + n N_b A_b \quad (17)$$

where  $m = 6$  = friction coefficient,  $n = 40$  = base coefficient,  $N_s$  is SPT blow count along the pile shaft,  $N_b$  is the SPT blow count at pile base;  $A_s$  is the pile skin area and  $A_b$  is the pile base cross sectional area.

Based on this approximate SPT formulas commonly adopted in Jakarta practice, the ultimate bearing capacity of the same pile size found is:

$$Q_{ult\_SPT} = 30,610 \text{ kN}$$

It can be seen the PMT and the SPT results give similar values of estimated pile axial capacity.

## 6. CONCLUDING REMARK

To derived  $c$  and  $\phi$  values of Jakarta stiff clay from PMT data, Meci model needs to be modified. The deformation modulus need to be divided into two parts as written in Equation (8a) and (8b). With this modified E function, cavity expansion theory can then be applied to derive the shear strength parameters.

PMT test in Jakarta stiff clay initially exhibits partially drained condition and then gradually become fully drained condition when reaching and beyond its yield pressure. The  $c$  and  $\phi$  values obtained from Pressuremeter test are effective stress parameters. The Pressuremeter test can reveal the effect of cementation of Jakarta stiff clay which appear in a higher value of cohesion which cannot be captured by triaxial test due to the difficulty in obtaining a good 'really' undisturbed Jakarta stiff clay samples by normal thin wall tube sampler.

The axial pile bearing capacity calculated by finite element method with strength and stiffness parameters derived from PMT test is comparable with the calculated bearing capacity of SPT formula commonly used in Jakarta's practice.

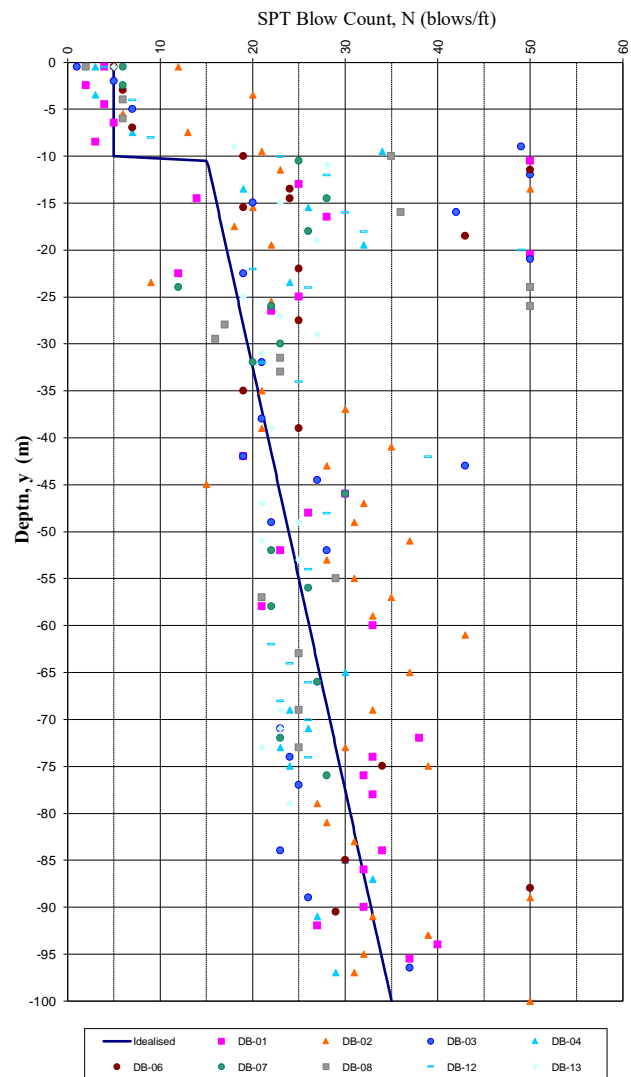


Figure 21 Idealized SPT Blow Counts

Further research is necessary to make sure whether the theory derived in this study can be applied to estimate the strength parameters of other soil types. It will be good if PMT test data can be done in conjunction with instrumented pile load test data tested to failure, with this the theory can be further verified.

## 7. ACKNOWLEDGEMENT

The author would like to thank Prof. Paulus. P. Rahardjo, and Prof. A. Aziz Djajaputra for their valuable guidance during the research. To Prof. H. Moeno, R. Karlinsari PhD and S. Herina, for their feedbacks. To GEC and PT. Pondasi Kisocon Raya for providing necessary data for the research. Finally, high appreciation also attributed to Universitas Katolik Parahyangan for facilitating the research.

## 8. REFERENCES

- Baguelin, F., Jezequel, J.F., Lemee, E., and Le Mehaute, A. (1972) "Expansion of Cylindrical Probes in Cohesive Soils", JSMFE, ASCE, 98; SM11. Proc. Paper 9377, pp1129-1142.
- Baguelin, F., Jezequel, J.F., and Shields, D.H. (1978) The Pressuremeter and Foundation Engineering, Trans Tech Publication, Switzerland.
- Briaud, J.L. (1992) The Pressuremeter, A.A. Balkema, Rotterdam.
- Briaud, J.L. (2013) Geotechnical Engineering: Unsaturated and Saturated Soils, John Wiley & Sons, New Jersey, USA.

- Clarke, B.G. (1995) *Pressuremeters in Geotechnical Design*, Blackie Academic and Professional, London.
- Clayton, R.I., Simons, N.E., and Matthews, M.C. (1982) *Site Investigation A Handbook for Engineers*, Granada Publishing, London
- Gambin, M. (1980) "A Review of the Menard Pressuremeter over the Last Twenty Years in Europe", *Sol Soils*, 32, Paris.
- Gambin, M. (1995) "Reasons for the Success of Menard Pressuremeter", *Proceedings of Fourth International Symposium on Pressuremeters*, May 17-19, 1995, Sherbrooke, Quebec, Canada.
- Gambin, M. and Frank, R. (2009) "Direct Design Rules for Piles using Menard Pressuremeter Test", *Foundation Design with Menard Pressuremeter Test, French Contributions to International Foundation Congress & Equipment, Expo '09*, pp3-10; also in *ASCE Geotechnical Special Publication no. 186*, pp111-118.
- Ghionna, v., et al. (1981) *Performance of Self-boring Pressuremeter Tests in Cohesive Deposits*, Report FHWA/RD-81/173/1981, MIT, Boston.
- Gouw, Tjie-Liong (2017) *Shear Strength Derivation of Jakarta Stiff Clay by Use of Pressuremeter Test based on Modified Cavity Expansion Theory*, PhD Dissertation, Universitas Katolik Parahyangan, Bandung, Indonesia.
- Mecsi, J. (2013) *Geotechnical Engineering Examples and Solutions Using the Cavity Expanding Theory*, Hungarian Geotechnical Society, Hungary.
- SNI 8460:2017 (2017). *Standar Nasional Indonesia - Persyaratan perancangan geoteknik*. Badan Standardisasi Nasional.